Article

Cyclic Peptide Inhibitors of Staphylococcal Virulence Prepared by Fmoc-Based Thiolactone Peptide Synthesis

Elizabeth A. George, Richard P. Novick, and Tom W. Muir

J. Am. Chem. Soc., **2008**, 130 (14), 4914-4924 • DOI: 10.1021/ja711126e

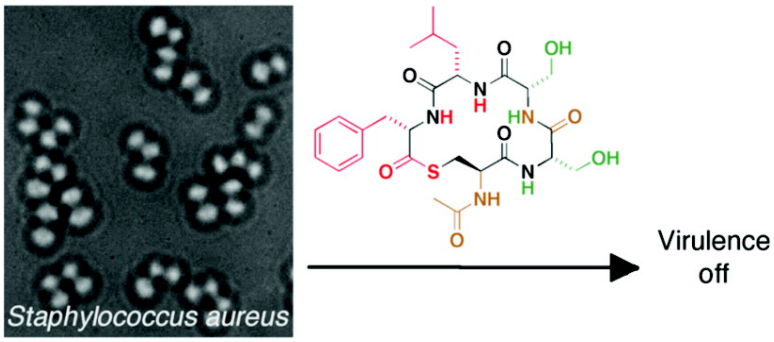

More About This Article

Additional resources and features associated with this article are available within the HTML version:

- Supporting Information
- Links to the 3 articles that cite this article, as of the time of this article download
- Access to high resolution figures
- Links to articles and content related to this article
- Copyright permission to reproduce figures and/or text from this article

View the Full Text HTML

J|A|C|S
ARTICLES
Published on Web 03/12/2008

Cyclic Peptide Inhibitors of Staphylococcal Virulence Prepared by Fmoc-Based Thiolactone Peptide Synthesis

Elizabeth A. George,[†] Richard P. Novick,[‡] and Tom W. Muir*,[†]

The Laboratory of Synthetic Protein Chemistry, Rockefeller University, New York, New York 10065, and Tri-institutional Training Program in Chemical Biology, Skirball Institute, Department of Microbiology, New York University Medical Center, New York, New York 10016

Received December 14, 2007; E-mail: muirt@rockefeller.edu

Abstract: Virulence factor production in *Staphylococcus aureus* is largely under the control of the accessory gene regulator (*agr*) quorum sensing system. There are four *agr* groups, all of which exhibit bacterial interference: each *agr* type synthesizes a cyclic autoinducing peptide (AIP) with a distinct sequence that activates its cognate AgrC receptor and inhibits activation of others. To better understand inhibitory AIP−AgrC interactions, we aimed to identify the minimal molecular determinants required to inhibit both non-cognate and cognate receptors. This minimization of the AIP pharmacophore also may have therapeutic relevance as the use of native AIPs to block virulence of non-cognate *agr* strains can prevent the establishment of an infection in vivo. We synthesized and evaluated the inhibitory activities of 10 AIP derivatives based on a truncated AIP analogue that inhibits all four *agr* types. To carry out the rapid, parallel synthesis of these peptides, we employed a new linker for Fmoc-based thioester peptide synthesis. Our results identify key structural elements that are necessary for AgrC inhibition and reveal key differences between non-cognate and cognate inhibitory requirements.

Introduction

The induction of virulence in *Staphylococcus aureus* is largely controlled by a quorum sensing system encoded by the accessory gene regulator (*agr*) operon.[1] AgrC, a receptor histidine kinase, is activated upon binding to a cognate autoinducing peptide (AIP), which facilitates the expression of downstream virulence factors. There are many *agr* polymorphisms among staphylococci, including four within *S. aureus*, resulting in four *agr* specificity groups with distinct AIP and AgrC sensor domain sequences (Figure 1A). Remarkably, most cross-group AIP−AgrC interactions are inhibitory, and although the physiological relevance of this phenomenon is still under investigation, it is a powerful tool used in the study of the *agr* system and has therapeutic potential.[2−4]

The four *S. aureus* AIPs are seven to nine amino acids long and all contain a thiolactone macrocycle, involving a conserved cysteine sulfhydryl group and the α-carboxylate, and an N-terminal tail region (Figure 1B). Previous structure−activity relationship (SAR) studies identified the hydrophobic character of the two C-terminal amino acids, which are highly conserved across all staphylococcal AIPs, as an essential element for both agonism and antagonism of AgrC.[5] However, the AIPs also contain activity determinants within either the tail region or the macrocycle, depending on the group, that are required for full activation of the receptor.[3,6,7] While agonism is very sensitive to changes in the AIP sequence, the antagonistic activities of

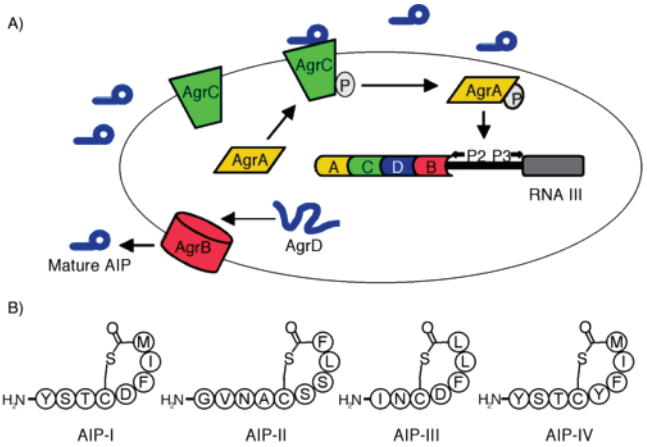

Figure 1. *agr* quorum sensing system. (A) AgrD is a propeptide that is processed and secreted, in part, by AgrB to form the mature AIP. Once a threshold AIP concentration is reached, the AIP molecules bind and activate their target receptor histidine kinase, AgrC, triggering autophosphorylation and phosphoryl transfer. AgrC transduces the signal to the response regulator AgrA, which goes on to activate transcription of the *agr* locus and of the effector molecule, RNAIII. (B) Structures and sequences of the AIPs of each of the four *S. aureus agr* groups.

[†] Rockefeller University.
[‡] New York University Medical Center.

(1) George, E. A.; Muir, T. W. *ChemBioChem* **2007**, *8*, 847.
(2) (a) Ji, G.; Beavis, R.; Novick, R. P. *Science (Washington, DC, U.S.)* **1997**, *276*, 2027. (b) Wright, J. W.; Jin, R.; Novick, R. P. *Proc. Natl. Acad. Sci. U.S.A.* **2005**, *102*, 1691. (c) Fleming, V.; Feil, E.; Sewell, A. K.; Day, N.; Buckling, A.; Massey, R. C. *J. Bacteriol.* **2006**, *188*, 7686.
(3) Mayville, P.; Ji, G.; Beavis, R.; Yang, H.; Goger, M.; Novick, R. P.; Muir, T. W. *Proc. Natl. Acad. Sci. U.S.A.* **1999**, *96*, 1218.
(4) Lyon, G. J.; Mayville, P.; Muir, T. W.; Novick, R. P. *Proc. Natl. Acad. Sci. U.S.A.* **2000**, *97*, 13330.
(5) Wright, J. S., III; Lyon, G. J.; George, E. A.; Muir, T. W.; Novick, R. P. *Proc. Natl. Acad. Sci. U.S.A.* **2004**, *101*, 16168.
(6) Lyon, G. J.; Wright, J. S.; Muir, T. W.; Novick, R. P. *Biochemistry* **2002**, *41*, 10095.

10.1021/ja711126e CCC: $40.75

Chart 1. Truncated AIP-II (trAIP-II) (**1**) and the Ten Analogues Synthesized and Tested in This Study[a]

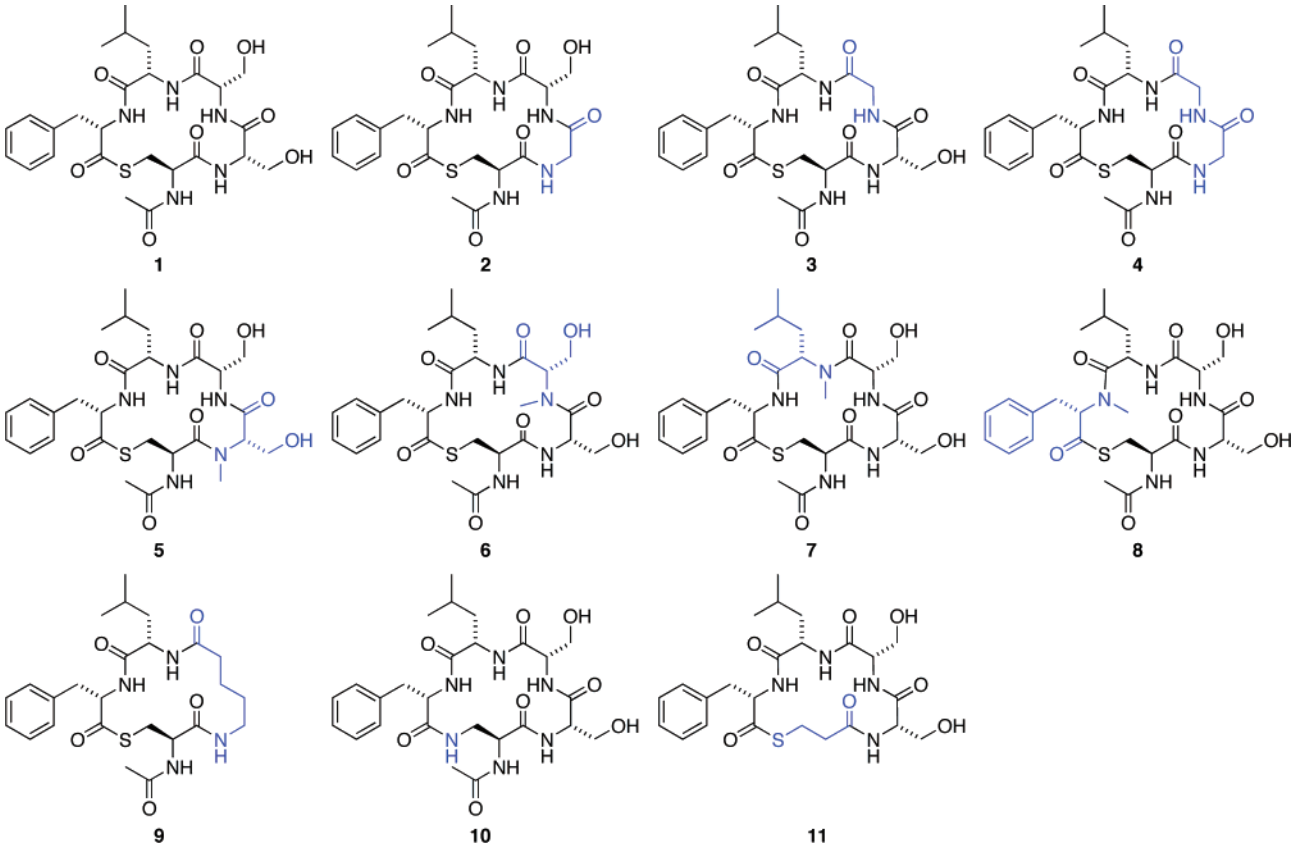

[a] Changes in each analogue relative to **1** are in blue.

the full-length, native AIPs seem to be fairly robust, being broadly tolerant to substitutions and truncations.[3−6,8] Furthermore, certain modifications convert an AIP to an antagonist of the cognate AgrC while maintaining inhibition of all non-cognate receptors. For example, and of relevance to the current study, truncation of the four tail residues of AIP-II (to give trAIP-II, **1**) converts the peptide into a potent global inhibitor of all four *agr* groups.[4]

To understand more fully the differences between agonism and antagonism in the AIP−AgrC interaction, we sought to discover the minimal determinants of AgrC inhibition. We synthesized 10 AIP-II analogues (Chart 1) based on the trAIP-II (**1**) scaffold to test the importance of the inhibition of the peptide backbone, side chains, thiolactone linkage, and N-terminus. To facilitate rapid, parallel synthesis of the AIPs, we also developed a new Fmoc-based AIP synthesis that is generally useful for the preparation of α-thioester peptides. The inhibitory activities of the trAIP-II analogues were tested against both AgrC-II and AgrC-I to compare trends for cognate and non-cognate inhibition. This SAR analysis led to the identification of a minimal pharmacophore structure with a reduced peptidic character that retains the antagonism of AgrC.

(7) McDowell, P.; Affas, Z.; Reynolds, C.; Holden, M. T.; Wood, S. J.; Saint, S.; Cockayne, A.; Hill, P. J.; Dodd, C. E.; Bycroft, B. W.; Chan, W. C.; Williams, P. *Mol. Microbiol.* **2001**, *41*, 503.
(8) (a) Otto, M.; Submuth, R.; Vuong, C.; Jung, G.; Gotz, F. *FEBS Lett.* **1999**, *450*, 257. (b) Scott, R. J.; Lian, L.; Muharram, S. H.; Cockayne, A.; Wood, S. J.; Bycroft, B. W.; Williams, P.; Chan, W. C. *Bioorg. Med. Chem. Lett.* **2003**, *13*, 2449. (c) Lyon, G. J.; Wright, J. S.; Christopoulos, A.; Novick, R. P.; Muir, T. W. *J. Biol. Chem.* **2002**, *277*, 6247.
(9) Schnolzer, M.; Alewood, P.; Jones, A.; Alewood, D.; Kent, S. B. *Int. J. Pept. Protein Res.* **1992**, *40*, 180.

Experimental Procedures

Materials. Amino acids, HBTU (2-(1H-Benzotriazole-1-yl)-1,1,3,3-tetramethyluronium hexafluorophosphate), HATU (2-(1H-7-Azabenzotriazol-1-yl)-1,1,3,3-tetramethyluronium hexafluorophosphate), PyBop (Benzotriazole-1-yl-oxy-tris-(dimethylamino)-phosphonium hexafluorophosphate), and Rink, and MBHA resins were purchased from Novabiochem (San Diego, CA) with the exceptions of Boc-*N*-methylphenylalanine (Fluka, Buchs, Switzerland) and Fmoc-DAPA(Boc)-OH (Neosystem Laboratoire, Strasbourg, France). All solvents were obtained from Fisher (Pittsburgh, PA), and trifluoroacetic acid was obtained from Halocarbon (River Edge, NJ). All other reagents were purchased from Sigma Aldrich (Milwaukee, WI).

Reversed-Phase HPLC and Mass Spectrometry. Analytical and semipreparative HPLC was performed using a Hewlett-Packard 1100 series instrument with diode array detection. A Vydac C_{18} column (5 μm, 4.6 mm × 150 mm) with a 1 mL/min flow rate was used for analytical scale HPLC, and a Vydac C_{18} column (10 μm, 10 mm × 250 mm) with a 4 mL/min flow rate was used for semipreparative HPLC. A Waters 2795 Separations Module plus 996 photodiode array detector with a Vydac C_{18} column (3 μm, 2.1 mm × 150 mm) and a 0.2 mL/min flow rate was used for LC-MS. In all cases, linear gradients of 0.1% aqueous TFA (solvent A) versus 90% acetonitrile, 10% water, and 0.1% TFA (solvent B) were utilized. ESI-MS was performed on a PE Sciex API-100 single quadrupole electrospray mass spectrometer. ESI-HRMS was performed on a Q-TOF Ultima hybrid quadrupole time-of-flight electrospray mass spectrometer (University of Illinois at Urbana−Champaign Mass Spectrometry Laboratory).

NMR Spectroscopy. Compounds **12**−**16** were dissolved in CD_3OD or $CDCl_3$, and ^1H and ^{13}C NMR spectra were recorded with a Bruker 400 MHz spectrometer. Measurements were taken at 298 K, and chemical shift values are relative to methanol (^1H 3.31 ppm, ^{13}C 49.00 ppm) or chloroform (^1H 7.26 ppm, ^{13}C 77.16 ppm). Peptides

1−**11** were dissolved in DMSO-d_6, and 1-D ^{1}H, homonuclear ^{1}H TOCSY, and ROESY experiments were performed on a Bruker 400 MHz spectrometer, Bruker 600 MHz spectrometer with cryoprobe, or Bruker Avance 700 MHz spectrometer with cryoprobe, respectively. The mixing times were 77 and 200 ms for TOCSY and ROESY experiments, respectively. In all cases, the sample temperature was 298 K, and the reported chemical shift values are relative to DMSO at 2.50 ppm. The chemical shift index (CSI) of each peptide was calculated using the formula

$$\mathrm{CSI} = \Sigma(|a\delta_i - \mathbf{1}\delta_i|)/n$$

where *a* is the peptide of interest, **1** is peptide **1**, *i* is the proton type (e.g., Cys1 NH), and *n* is the total number of protons included in the calculation. Protons directly bonded to the macrocyclic scaffold plus the exocyclic N-terminal amide proton were included in each CSI (Cys1 NH, αH, *β*H; Ser2 NH, αH; Ser3 NH, αH; Leu NH, αH; and Phe NH, αH). The protons of the modified residue(s) were excluded.

Synthesis. 3-*t*-Butyldisulfanyl-propane-1,2-diol (12). A solution containing 1-mercapto-ethane-1,2-diol (3.0 g, 27.7 mmol, 1.0 equiv), 2-methyl-propane-2-thiol (25 g, 277 mmol, 10.0 equiv), and triethylamine (7.0 g, 69.3 mmol, 2.5 equiv) dissolved in methanol (55 mL) was stirred at room temperature with bubbling O_2 overnight (>10 h). Methanol and excess 2-methyl-propane-2-thiol were removed in vacuo, and the crude product was purified by flash chromatography using 3:2 hexanes/ethyl acetate to give 5.4 g of **12** (99%) as a clear oil. ^{1}H NMR (400 MHz, CD_3OD) δ 3.83 (m, 1H), δ 3.58 (dd, 1H, J = 11.3, 4.8 Hz), δ 3.52 (dd, 1H, J = 11.3, 5.8 Hz), δ 2.90 (dd, 1H, J = 13.3, 5.3 Hz), δ 2.78 (dd, 1H, J = 13.3, 7.3 Hz), δ 1.34 (s, 9H); ^{13}C NMR (100 MHz, CD_3OD) δ 72.33, δ 65.90, δ 48.45, δ 45.64, δ 30.25, ESI-MS *m*/*z* calcd for $C_7H_{16}O_2S_2$ 196.3, found 393.0 ([2M + H$^+$]).

1,2-Bis-(*t*-butyl-dimethyl-silanyloxy)-3-*t*-butyldisulfanyl-propane (13). *t*-Butyl-chloro-dimethyl-silane (11 g, 72 mmol, 3.0 equiv), imidazole (9.8 g, 144 mmol, 6.0 equiv), and 4-dimethylaminopyridine (170 mg, 1.4 mmol, 0.06 equiv) were added on ice to a solution of **12** (4.7 g, 24 mmol, 1.0 equiv) dissolved in 240 mL of anhydrous DMF. The reaction was stirred under N_2 at room temperature overnight at which point 0.5 N NaOH was added to quench the reaction, and the product was extracted with ethyl acetate, washed with 1 N HCl, dried over Na_2SO_4, filtered, and dried in vacuo. Excess DMF was removed by an azeotrope with hexanes to yield 10 g (99%) of **13**, which was taken on to the next step without further purification. ^{1}H NMR (400 MHz, $CDCl_3$) δ 3.89 (m, 1H), δ 3.61 (dd, 1H, J = 10.1, 5.0 Hz), δ 3.53 (dd, 1H, J = 10.1, 6.3 Hz), δ 2.99 (dd, 1H, J = 13.1, 4.9 Hz), δ 2.73 (dd, 1H, J = 13.1, 6.7 Hz), δ 1.33 (s, 9H), δ 0.90 (s, 18H), δ 0.08 (m, 12H); ^{13}C NMR (100 MHz, $CDCl_3$) δ 72.70, 66.40, 47.81, 46.00, 30.06, 26.10, 26.04, 25.86, 25.82, 18.50, 18.30, −2.79, −3.41, −4.39, −4.20, −5.20, −5.18, ESI-MS *m*/*z* calcd for $C_{19}H_{44}O_2S_2Si_2$ 424.2, found 423.0 ([M$^-$]).

2-(*t*-Butyl-dimethyl-silanyloxy)-3-*t*-butyldisulfanyl-propan-1-ol (14). A cold 1:1 mixture of TFA and water (18 mL) was added dropwise to a solution of **13** (4.4 g, 10 mmol, 1.0 equiv) in 45 mL of THF. The reaction was stirred at 0 °C for 4.5 h, and then it was slowly poured into a separation funnel containing an ice cold solution of $NaHCO_3$ to bring the pH above 7. The product was extracted with ethyl acetate, washed with water and brine, dried over Na_2SO_4, and filtered, and the solvents were removed in vacuo. Purification by flash chromatography with 15:1 hexanes/ethyl acetate yielded 2.0 g (65%) of **14**. ^{1}H NMR (400 MHz, CD_3Cl) δ 3.97 (m, 1H), δ 3.70 (dd, 1H, J = 11.3, 3.5 Hz), δ 3.62 (dd, 1H, J = 11.3, 4.0 Hz), δ 2.87 (dd, 1H, J = 13.4, 7.2 Hz), δ 2.79 (dd, 1H, J = 13.4, 5.4 Hz), δ 1.34 (s, 9H), δ 0.91 (s, 9H), δ 0.13 (s, 3H), δ 0.10 (s, 3H); ^{13}C NMR (100 MHz, $CDCl_3$) δ 72.14, 65.01, 48.06, 44.05, 29.98, 25.93, 18.19, −4.29, −4.48, −4.62, ESI-MS *m*/*z* calcd for $C_{13}H_{30}O_2S_2Si_2$ 310.2, found 309.0 ([M$^-$]).

2-(*t*-Butyl-dimethyl-silanyloxy)-3-*t*-butyldisulfanyl-propionaldehyde (15). Dess−Martin periodinane (1.3 g, 3.1 mmol, 1.2 equiv) was added to a solution of **14** (800 mg, 2.6 mmol, 1.0 equiv) in 26 mL of CH_2Cl_2 under N_2. The reaction was stirred at room temperature for 2 h, then diluted with CH_2Cl_2 and ethyl acetate. The product was washed with 0.1 N HCl, 1 N NaOH, and brine, dried over Na_2SO_4, and filtered, and the solvents were removed in vacuo. Purification by flash chromatography using 19:1 hexanes/ethyl acetate yielded 590 mg (73%) of **15**. ^{1}H NMR (400 MHz, $CDCL_3$) δ 9.64 (s, 1H), δ 4.22 (m, 1H), δ 2.99 (dd, 1H, J = 13.4, 4.2 Hz), δ 2.80 (dd, 1H, J = 13.4, 7.9 Hz), δ 1.31 (s, 9H), δ 0.91 (s, 9H), δ 0.12 (s, 3H), δ 0.10 (s, 3H); ^{13}C NMR (100 MHz, $CDCl_3$) δ 202.17, 76.57, 48.22, 43.66, 29.97, 25.84, 18.30, −4.55, −4.63, ESI-MS *m*/*z* calcd for $C_{13}H_{28}O_2S_2Si$ 308.1, found 309.0 ([M + H$^+$]).

2-(*t*-Butyl-dimethyl-silanyloxy)-3-*t*-butyldisulfanyl-propionic Acid (16). Compound **15** (227 mg, 0.74 mmol, 1.0 equiv) was dissolved in 4 mL of *t*-butyl alcohol. 2-Methyl-2-butene (3.02 g, 42.9 mmol, 58 equiv) was added to the solution on ice, followed by a pre-dissolved solution of monobasic sodium phosphate (225 mg, 1.63 mmol, 2.2 equiv) and 80% sodium chlorite (251 mg, 2.22 mmol, 3.0 equiv) in water (4 mL). The reaction was stirred vigorously to ensure mixing of the two phases at room temperature for 2 h. The reaction mixture was diluted with ethyl acetate, washed with 0.1 N HCl and brine, dried over Na_2SO_4, and filtered, and the solvents were removed in vacuo. Purification by flash chromatography using 19:1 CH_2Cl_2/methanol yielded 160 mg (66%) of **16** as a clear oil. ^{1}H NMR (400 MHz, $CDCL_3$) δ 4.47 (m, 1H), δ 3.12 (dd, 1H, J = 13.4, 3.6 Hz), δ 2.93 (dd, 1H, J = 13.4, 7.9 Hz), δ 1.33 (s, 9H), δ 0.92 (s, 9H), δ 0.15 (s, 3H), δ 0.13 (s, 3H); ^{13}C NMR (100 MHz, $CDCl_3$) δ 176.60, 71.27, 48.23, 45.77, 30.00, 25.82, 18.29, −4.80, −4.86, ESI-HRMS *m*/*z* calcd for $C_{13}H_{28}O_3S_2Si$ [M + H$^+$] 325.1327, found 325.1329.

Fmoc AIP Synthesis. Peptides **1**−**7**, **9**, and **11** were manually synthesized. Linker **16** (188 mg, 0.61 mmol, 1.1 equiv relative to resin substitution) was added to a solution of HBTU (207 mg, 0.55 mmol, 1.0 equiv relative to resin loading) in DMF (1.2 mL), followed by DIEA (diisopropylethylamine) (0.25 mL, 1.44 mmol, 2.6 equiv relative to resin) to pre-activate the acid. After 3 min, the solution was added to Rink amide resin and stirred by bubbling N_2 through the vessel at room temperature for 4 h. Remaining free amines were acetylated by two treatments with a 1:1:8 solution of acetic anhydride/DIEA/DMF for 10 min. Deprotection of the TBS group was accomplished by the addition of tetrabutyl ammonium fluoride (10 mL of a 1.0 M solution in THF) overnight at room temperature. 4-Dimethylaminopyridine (0.1 equiv relative to phenylalanine) was used in addition to HBTU and DIEA to double couple phenylalanine to the hydroxyl group of the linker. Subsequent steps were completed with standard HBTU/DIEA activation and piperidine deprotection protocols for Fmoc solid-phase peptide chemistry with a few exceptions. N-Methylated amino acids were double coupled, once with HBTU and once with HATU. Other unnatural monomers (Fmoc-5-amino-pentanoic acid in **9** and 3-trityl-sulfanyl-propionic acid in **11**) were coupled with standard methods. Finally, all peptides, with the exception of **11**, were acetylated at the N-terminus with a 1:1:8 solution of acetic anhydride/DIEA/DMF for 10 min. Each peptide was cleaved from the solid support by treatment with 95:2.5:2.5 TFA/TIS/water for 3−4 h at room temperature, followed by filtration and washing of the beads with the TFA cleavage cocktail. The peptides were either purified by semipreparative HPLC or taken on to the cyclization step without purification.

The cyclization buffer contained 20% acetonitrile and 80% 6 M guanidinium chloride in 0.1 M sodium phosphate buffer pH 6.5. TCEP (tris-(2-carboxy)ethyl phosphine) (70 mM) was added to this solution, and the pH was brought back up to 6.6−6.8 with 4 M NaOH. Each linear peptide was dissolved in this solution to a final concentration of 100 μM and rocked at room temperature for 2−24 h, and the reaction was monitored by analytical HPLC. The desired AIP product was then purified by semipreparative HPLC.

Data for Peptide 1. ^{1}H NMR (400 MHz, DMSO-d_6) δ 8.68 (d, 1H, J = 8.8 Hz), δ 8.46 (d, 1H, J = 8.2 Hz), δ 8.12 (m, 2H), δ 7.60 (d,

1H, $J = 8.7$ Hz), δ 7.25 (m, 2H), δ 7.21 (m, 3H), δ 5.12 (t, 1H, $J =$ 5.4 Hz), δ 5.03 (t, 1H, $J = 5.4$ Hz), δ 4.56 (m, 1H), δ 4.39 (m, 1H), δ 4.28 (m, 1H), δ 4.22 (m, 1H), δ 3.92 (m, 1H), δ 3.64 (m, 1H), δ 3.58 (m, 2H), δ 3.52 (m, 1H), δ 3.31 (obsc 1H), δ 3.16 (m, 1H), δ 2.84 (m, 2H), δ 1.86 (s, 3H), δ 1.38 (m, 1H), δ 1.30 (m, 1H), δ 1.22 (m, 1H), δ 0.74 (d, 3H, $J = 6.3$ Hz), δ 0.71 (d, 3H, $J = 6.3$ Hz), ESI-MS *m*/*z* calcd for $C_{26}H_{37}N_5O_8S$ 579.2, found 580.0 ([M + H^+]).

Data for Peptide 2. ^{1}H NMR (400 MHz, DMSO-d_6) δ 8.67 (d, 1H, $J = 9.0$ Hz) δ 8.44 (d, 1H, $J = 7.9$ Hz), δ 8.21 (m, 1H), δ 7.99 (d, 1H, $J = 7.7$ Hz), δ 7.59 (d, 1H, $J = 8.3$ Hz), δ 7.26 (m, 2H), δ 7.20 (m, 3H), δ 5.21 (t, 1H, $J = 5.5$ Hz), δ 4.59 (m, 1H), δ 4.32 (m, 1H), δ 4.21 (m, 1H), δ 3.98 (m, 1H), δ 3.89 (m, 1H), δ 3.62 (m, 1H), δ 3.52 (m, 1H), δ 3.32 (obsc, 1H), δ 3.31 (obsc, 1H), δ 3.16 (m, 1H), δ 2.84 (m, 2H), δ 1.86 (s, 3H), δ 1.31 (m, 2H), δ 1.18 (m, 1H), δ 0.74 (d, 3H, $J = 6.2$ Hz), δ 0.69 (d, 3H, $J = 6.2$ Hz), ESI-MS *m*/*z* calcd for $C_{25}H_{35}N_5O_7S$ 549.2, found 550.0 ([M + H^+]).

Data for Peptide 3. ^{1}H NMR (400 MHz, DMSO-d_6) δ 8.46 (m, 1H), δ 8.36 (d, 1H, $J = 7.4$ Hz), δ 8.30 (d, 1H, $J = 8.0$ Hz), δ 8.02 (m, 2H), δ 7.24 (m, 5H), δ 4.64 (m, 1H), δ 4.41 (m, 2H), δ 3.99 (m, 1H), δ 3.79 (dd, 1H, $J = 14.0$, 3.6 Hz), δ 3.57 (m, 3H), δ 3.35 (obsc, 1H), δ 3.13 (m, 1H), δ 2.91 (m, 1H), δ 2.62 (m, 1H), δ 1.86 (s, 3H), δ 1.49 (m, 1H), δ 1.12 (m, 2H), δ 0.78 (d, 3H, $J = 6.5$ Hz), δ 0.71 (d, 3H, $J = 6.5$ Hz); ESI-MS *m*/*z* calcd for $C_{25}H_{35}N_5O_7S$ 549.2, found 550.0 ([M + H^+]).

Data for Peptide 4. ^{1}H NMR (400 MHz, DMSO-d_6) δ 8.39 (m, 1H) δ 8.29 (m, 2H), δ 8.15 (d, 1H, $J = 9.4$ Hz), δ 8.08 (m, 1H), δ 7.23 (m, 5H), δ 4.67 (m, 1H), δ 4.42 (m, 1H), δ 4.10 (m, 1H), δ 3.98 (m, 1H), δ 3.79 (m, 1H), δ 3.58 (dd, 1H, $J = 14.2$, 6.4 Hz), δ 3.28 (obsc, 1H), δ 3.18 (m, 1H), δ 2.87 (m, 1H), δ 2.72 (m, 1H), δ 1.86 (s, 3H), δ 1.43 (m, 2H), δ 1.10 (m, 1H), δ 0.78 (d, 3H, $J = 6.5$ Hz), δ 0.71 (d, 3H, $J = 6.5$ Hz); ESI-MS *m*/*z* calcd for $C_{24}H_{33}N_5O_6S$ 519.2, found 520.3 ([M + H^+]).

Data for Peptide 5. ^{1}H NMR (400 MHz, DMSO-d_6) δ 8.73 (d, 1H, $J = 8.3$ Hz), δ 8.56 (d, 1H $J = 9.0$ Hz), δ 7.98 (d, 1H $J = 7.4$ Hz), δ 7.49 (d, 1H, $J = 8.1$ Hz), δ 7.25 (m, 2H), δ 7.18 (m, 3H), δ 5.25 (m, 1H), δ 4.95 (m, 3H), δ 4.38 (m, 1H), δ 4.16 (m, 1H), δ 4.08 (m, 1H), δ 3.80 (m, 1H), δ 3.73 (m, 2H), δ 3.33 (obsc, 1H), δ 3.12 (m, 1H), δ 3.00 (s, 3H), δ 2.90 (m, 1H), δ 2.83 (m, 1H), δ 1.87 (s, 3H), δ 1.26 (m, 3H), δ 0.73 (m, 6H); ESI-MS *m*/*z* calcd for $C_{27}H_{39}N_5O_8S$ 593.3, found 595.0 ([M + H^+]).

Data for Peptides 6a and 6b. (The cis and trans amide isomers were ~50% each.) ^{1}H NMR (400 MHz, DMSO-d_6) δ 8.66 (d, 1H, $J =$ 7.4 Hz), δ 8.47 (d, 1H, $J = 7.6$ Hz), δ 8.24 (d, 1H, $J = 8.6$ Hz), δ 8.10 (m, 3H), δ 7.48 (m, 2H), δ 7.25 (m, 5H), δ 7.14 (m, 5H), δ 4.90 (m, 1H), δ 4.83 (m, 1H), δ 4.59 (m, 1H), δ 4.51 (m, 1H), δ 4.45 (m, 1H), δ 4.35 (m, 1H), δ 4.26 (m, 1H), δ 4.12 (m, 2H), δ 3.99 (m, 1H), δ 3.88 (m, 1H), δ 3.77 (m, 1H), δ 3.63 (m, 1H), δ 3.56 (m, 3H), δ 3.34 (obsc, 1H), δ 3.29 (obsc, 1H), δ 3.26 (obsc, 1H), δ 3.24 (obsc, 1H), δ 3.14 (m, 2H), δ 3.02 (m, 1H), δ 2.97 (m, 2H), δ 2.66 (s, 6H), δ 2.49 (obsc, 1H), δ 1.86 (s, 6H), δ 1.39 (m, 5H), δ 1.29 (m, 1H), δ 0.77 (m, 6H), δ 0.73 (m, 6H); ESI-MS *m*/*z* calcd for $C_{27}H_{39}N_5O_8S$ 593.3, found 595.0 ([M + H^+]).

Data for Peptide 7. ^{1}H NMR (400 MHz, DMSO-d_6) δ 8.45 (d, 1H, $J = 8.2$ Hz), δ 8.25 (d, 1H, $J = 9.9$ Hz), δ 8.05 (d, 1H, $J = 8.5$ Hz), δ 7.76 (d, 1H, $J = 9.1$ Hz), δ 7.25 (m, 3H), δ 7.21 (m, 2H), δ 5.15 (m, 1H), δ 4.82 (m, 1H), δ 4.75 (m, 1H), δ 4.67 (m, 1H), δ 4.44 (m, 1H), δ 4.22 (m, 1H), δ 3.63 (m, 2H), δ 3.50 (m, 1H), δ 3.45 (m, 1H), δ 3.37 (obsc, 1H), δ 3.36 (obsc, 1H), δ 3.11 (m, 1H), δ 3.01 (s, 3H), δ 2.89 (m, 1H), δ 2.70 (m, 1H), δ 1.90 (m, 1H), δ 1.85 (s, 3H), δ 1.37 (m, 1H), δ 1.25 (m, 1H), δ 0.75 (d, 3H, $J = 6.5$ Hz), δ 0.69 (d, 3H, $J = 6.4$ Hz); ESI-MS *m*/*z* calcd for $C_{27}H_{39}N_5O_8S$ 593.3, found 595.0 ([M + H^+]).

Data for Peptide 9. ^{1}H NMR (400 MHz, DMSO-d_6) δ 8.24 (d, 1H, $J = 7.8$ Hz), δ 8.09 (m, 1H), δ 7.94 (d, 1H, $J = 8.9$ Hz), δ 7.74 (d, 1H, $J = 9.2$ Hz), δ 7.26 (m, 3H), δ 7.20 (m, 2H), δ 4.67 (m, 1H), δ 4.34 (m, 1H), δ 4.20 (m, 1H), δ 3.43 (m, 1H), δ 3.28 (obsc, 1H), δ 3.21 (obsc, 1H), δ 2.90 (m, 1H), δ 2.76 (m, 2H), δ 2.11 (m, 1H), δ 2.01 (m, 1H), δ 1.84 (s, 3H), δ 1.50 (m, 3H), δ 1.32 (m, 1H), δ 1.20 (m, 2H), δ 0.97 (m, 1H), δ 0.75 (d, 3H, $J = 6.5$ Hz), δ 0.68 (d, 3H, $J = 6.5$ Hz); ESI-MS *m*/*z* calcd for $C_{25}H_{36}N_4O_5S$ 504.2, found 505.0 ([M + H^+]).

Data for Peptide 11. ^{1}H NMR (400 MHz, DMSO-d_6) δ 8.76 (d, 1H, $J = 8.4$ Hz), δ 8.18 (d, 1H, $J = 7.5$ Hz), δ 8.06 (d, 1H, $J = 7.8$ Hz), δ 7.34 (d, 1H, $J = 8.7$ Hz), δ 7.26 (m, 3H), δ 7.20 (m, 2H), δ 5.09 (t, 1H, $J = 5.0$ Hz), δ 4.98 (t, 1H, $J = 5.3$ Hz), δ 4.54 (m, 1H), δ 4.26 (m, 1H), δ 4.18 (m, 1H), δ 3.88 (m, 1H), δ 3.64 (m, 4H), δ 3.33 (obsc, 1H), δ 3.21 (m, 1H), δ 2.85 (m, 2H), δ 2.62 (obsc, 1H), δ 2.34 (m, 1H), δ 1.42 (m, 1H), δ 1.24 (m, 2H), δ 0.74 (d, 3H, $J = 6.3$ Hz), δ 0.70 (d, 3H, $J = 6.3$ Hz); ESI-MS *m*/*z* calcd for $C_{24}H_{34}N_4O_7S$ 522.2, found 523.0 ([M + H^+]).

trAIP-II Lactam (10) Synthesis. The peptide was synthesized similarly to the full-length AIP-II lactam.[3] Chain elongation was completed using Fmoc SPPS protocols. Fmoc-serine(benzyl)-OH was used in residue positions two and three. Fmoc-DAPA(Boc)-OH was used in place of cysteine. Once cleaved from the resin with TFA, the partially protected linear peptide was cyclized with PyBop and DIEA, purified by semipreparative HPLC, and treated with 25:1 HF/4-methylphenol (*p*-cresol) for 1 h at 0 °C to remove the benzyl groups. The final product was purified with semipreparative HPLC. ^{1}H NMR (400 MHz, DMSO-d_6) δ 8.67 (m, 1H), δ 8.11 (m, 1H), δ 8.04 (m, 1H), δ 7.72 (m, 1H), δ 7.59 (m, 1H), δ 7.49 (m, 1H), δ 7.20 (m, 5H), δ 4.38 (m, 2H), δ 4.31 (m, 1H), δ 3.94 (m, 1H), δ 3.84 (m, 1H), δ 3.79 (m, 1H), δ 3.71 (m, 1H), δ 3.62 (m, 3H), δ 3.21 (obsc, 1H), δ 3.00 (m, 1H), δ 2.85 (m, 1H), δ 1.84 (s, 3H), δ 1.37 (m, 1H), δ 1.25 (m, 1H), δ 1.10 (m, 1H), δ 0.76 (d, 3H, $J = 6.5$ Hz), δ 0.69 (d, 3H, $J = 6.2$ Hz); ESI-MS *m*/*z* calcd for $C_{26}H_{38}N_6O_8S$ 562.3, found 563.5 ([M + H^+]).

trAIP-II MeF (8) Synthesis. Manual solid-phase peptide synthesis with standard in situ neutralization/HBTU activation protocol for Boc chemistry[9] was used for chain elongation on a mercaptopropionamide MBHA resin. Leucine was double coupled to N-methylated phenylalanine with HBTU, then HATU. The peptide was cleaved from the resin by treatment with 25:1 HF/*p*-cresol for 1 h at 0 °C, precipitated, washed with diethyl ether, and purified by semipreparative HPLC. After lyophilization, the linear peptide was dissolved again in MeCN, water, and 0.1% TFA and cyclized in solution by the addition of a 4× volume of 0.1 M sodium phosphate buffer, pH 7, for 2 h at room temperature. The final AIP product was purified by semipreparative HPLC. ^{1}H NMR (400 MHz, DMSO-d_6) δ 8.50 (d, 1H, $J = 8.3$ Hz), δ 8.25 (d, 1H, $J =$ 8.6 Hz), δ 7.86 (d, 1H, $J = 9.2$ Hz), δ 7.80 (d, 1H, $J = 9.1$ Hz), δ 7.25 (m, 3H), δ 7.14 (m, 2H), δ 5.16 (m, 1H), δ 5.00 (m, 1H), δ 4.63 (m, 1H), δ 4.39 (m, 1H), δ 4.28 (m, 1H), δ 4.25 (m, 1H), δ 4.20 (m, 1H), δ 3.63 (m, 1H), δ 3.53 (m, 3H), δ 3.21 (obsc, 2H), δ 3.19 (obsc, 1H), δ 2.89 (m, 1H), δ 2.64 (s, 3H), δ 1.88 (s, 3H), δ 1.52 (m, 2H), δ 1.32 (m, 1H), δ 0.86 (d, 3H, $J = 6.0$ Hz), δ 0.81 (d, 1H, $J =$ 6.1 Hz); ESI-MS *m*/*z* calcd for $C_{27}H_{39}N_5O_8S$ 593.3, found 595.0 ([M + H^+]).

Inhibition Assays. The inhibitory activities of peptides **1**−**11** for *agr* activation were analyzed using a previously described assay with a β-lactamase reporter gene read-out.[6] Briefly, cell cultures of *agr*-null cell lines RN9222 (CA1-I) and RN9372 (CA2-II) with plasmids containing *agr*CA and *agr*-P3::*blaZ* were grown in CYGP to early exponential phase growth ($OD_{650} = 0.15-0.30$). The 80 μL aliquots were treated with 125 nM agonist AIP and varying concentrations of peptides **1**−**11** or buffer for 1 h with shaking at 37 °C in a THERMOmax microplate reader (Molecular Devices). Cell density was monitored by OD_{650} readings taken every 1 min. Immediately following Nitrocefin addition, hydrolysis was monitored by OD_{490} readings taken every 20 s over 20 min. All peptide stock solution concentrations were determined by amino acid analysis (AAA) at the Keck AAA and Protein Sequencing Lab (Yale University, New Haven, CT).

Scheme 1. General Routes for Synthesis of AIPs with Truncated AIP-II (**1**) Shown as an Example[a]

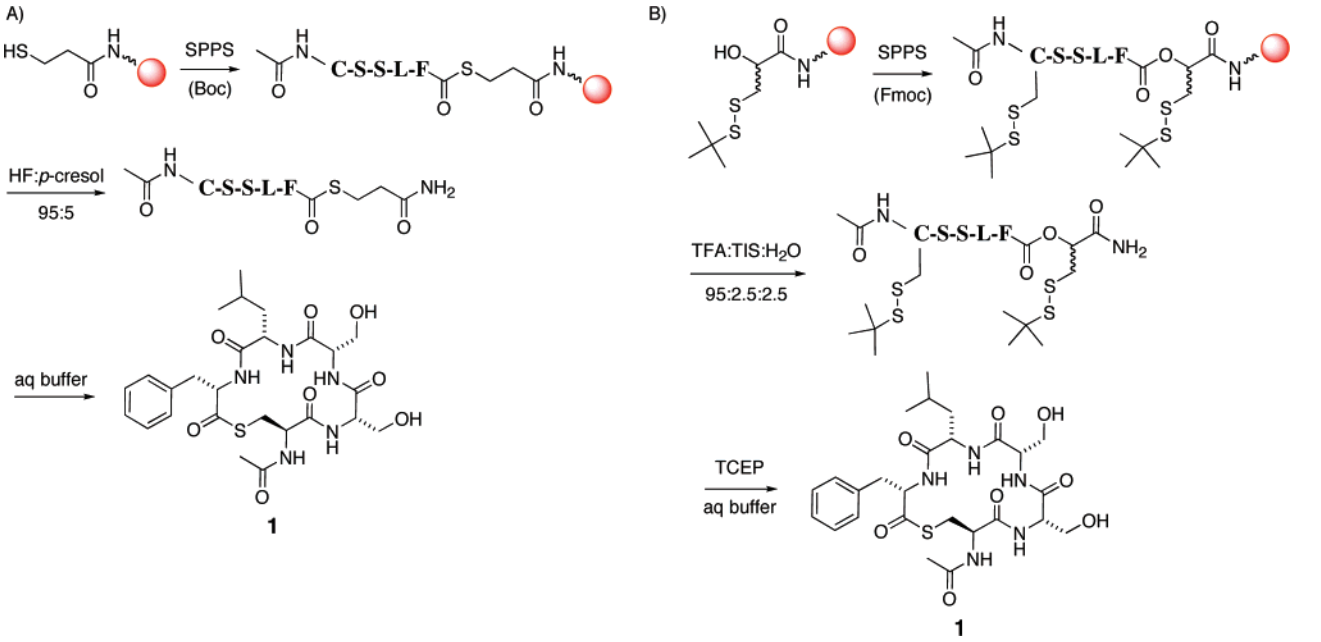

[a] (A) AIP synthesis using Boc chemistry.[6] The resin is modified with a thiol handle via a previously described method.[11] (B) Proposed Fmoc chemistry-based route to AIPs involving a latent thioester linker.[12]

Data Analysis. Assay data were plotted as initial β-lactamase hydrolysis velocity versus log peptide concentration. Error bars represent the standard deviation from the mean. The values obtained for initial velocity were normalized to cell density. The normalized data were analyzed using nonlinear regression and fit to a sigmoidal dose response curve using the PRISM 4.0 package (GraphPad Software, San Diego, CA). IC_{50} values were extracted from the Hill equation used for nonlinear regression analysis

$$E = \text{basal} + \frac{E_{max} - \text{basal}}{1 + 10^{((\log IC_{50} - \log[A])n_H)}}$$

in which E is the effect, [A] is the antagonist concentration, n_H is the midpoint slope, and E_{max} and basal are the upper and lower asymptotes, respectively.

Results

Design and Synthesis of trAIP-II Derivatives. To elucidate the minimal determinants of inhibition by trAIP-II, we set out to systematically perturb each structural aspect of the molecule (Chart 1). Previously, alanine scanning of full-length AIP-II showed that the two serine hydroxyl groups are not necessary for biological activity.[3] Guided by this observation, we designed trAIP-II analogues **2**−**4**, in which the serines were replaced with glycines either individually or in combination. Given that the hydrophobicity of the C-terminal residues is known to be required for biological activity,[5] the leucine and phenylalanine side chains were not perturbed in this study. Next, each amide in the macrocycle was N-methylated (**5**−**8**) to probe interactions involving the AIP backbone, which had yet to be evaluated in any AIP. To test as to whether these side-chain and backbone modifications could be combined, we completely removed the serines in peptide **9** and replaced them with a methylene linker derived from 5-aminopentanoic acid.

Previous SAR studies on full-length AIP-II revealed that the thiolactone linkage is a critical determinant in receptor activation, but, interestingly, not inhibition; a lactam analogue of AIP-II is a very poor agonist but potent antagonist of the *agr* response.[3] Thus, we designed a lactam (**10**) analogue to investigate as to whether the thiolactone linkage is necessary for inhibition in the context of truncated AIP-II. Last, to complete the structure−activity analysis, we designed peptide **11** in which the acetylated α-amino group of the cysteine was removed, allowing us to determine as to whether this vestige of the native AIP tail plays any role in the inhibitory activity of the peptide.

The standard AIP synthesis used in our laboratory involved a combined solid-phase, solution-phase route in which a linear unprotected peptide α-thioester, prepared by *t*-butoxy carbonyl (Boc) solid-phase peptide synthesis (SPPS), underwent cyclization through transthioesterification in aqueous solution (Scheme 1A).[6] Although this is an efficient synthetic route, the reliance on Boc-SPPS to generate the α-thioester precursor does create a bottleneck in the process, due to the need to use anhydrous HF in the cleavage step. In principle, the generation of peptide α-thioester precursors using Fmoc-SPPS would make feasible the parallel synthesis of many AIP analogues, thereby allowing more rapid structure−activity analysis of this system. However, the synthesis of α-thioester peptides via Fmoc-SPPS is a long-standing problem in peptide chemistry; and although many methods have been developed, none has gained widespread use owing to a variety of drawbacks, mainly a lack of generality or low yields (summarized in ref 10a,b).

In thinking about this problem, we were drawn to the latent thioester-linker work of Botti et al.[12] and Danishefsky et al.[13] In these methods, C-terminal thioesters were generated following an intramolecular O to S acyl shift. We imagined that the Botti

(10) (a) Muralidharan, V.; Muir, T. W. *Nat. Methods* **2006**, *3*, 429. (b) Camarero, J. A.; Mitchell, A. R. *Protein Pept. Lett.* **2005**, *12*, 723.
(11) Camarero, J. A.; Cotton, G. J.; Adeva, A.; Muir, T. W. *J. Pept. Res.* **1998**, *51*, 303.
(12) Botti, P.; Villain, M.; Manganiello, S.; Gaertner, H. *Org. Lett.* **2004**, *6*, 4861.
(13) Warren, J. D.; Miller, J. S.; Keding, S. J.; Danishefsky, S. J. *J. Am. Chem. Soc.* **2004**, *126*, 6576.

Scheme 2. (A) Synthesis of Linker **16**[a] and (B) Fmoc AIP Synthesis[b]

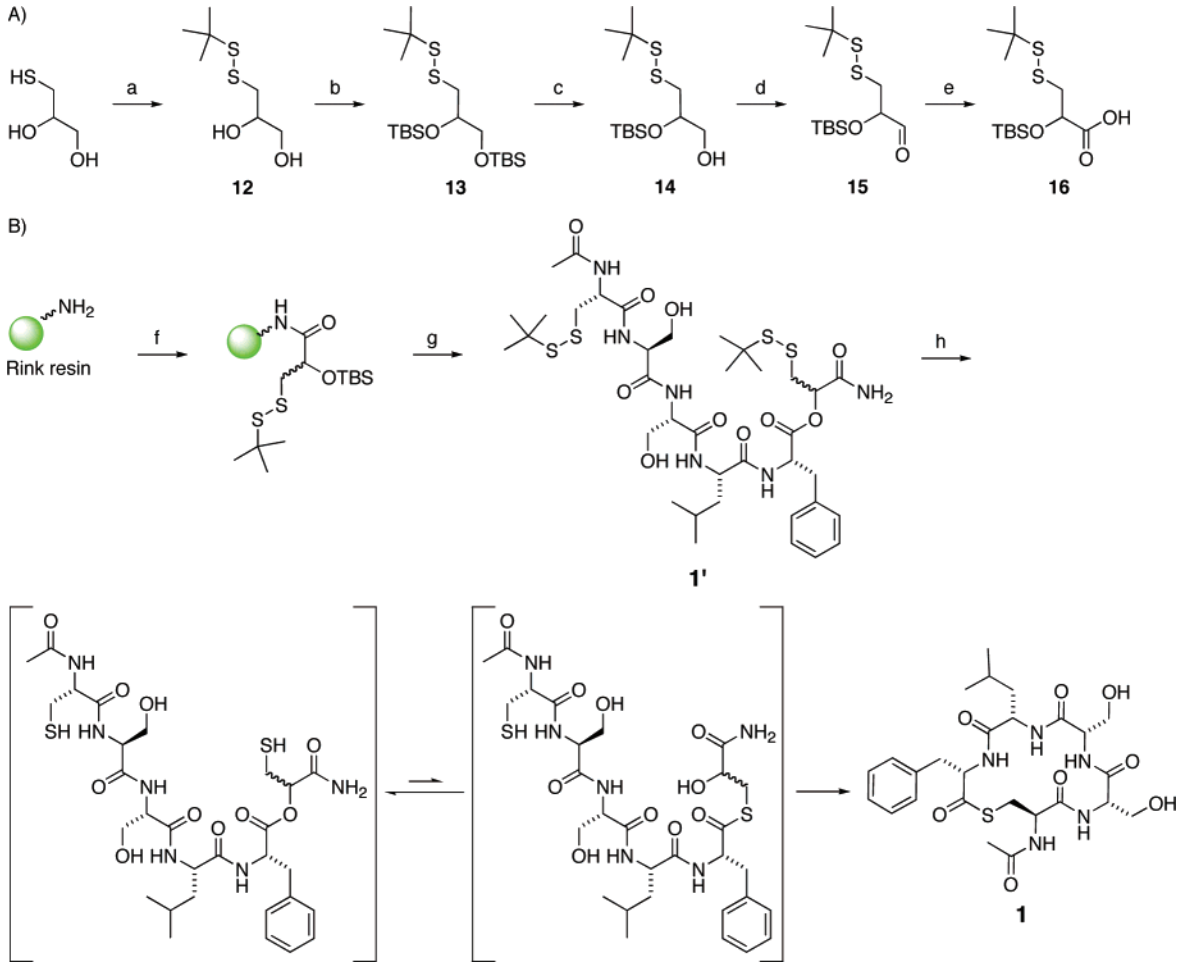

[a] Conditions: (a) *t*-butylthiol, TEA, O_2, MeOH, 99%; (b) TBSCl, imidazole, cat. DMAP, DMF, 99%; (c) TFA/H_2O 1:5, THF, 65%; (d) DMP, DCM, 73%; (e) NaOCl, 2-methyl-2-butene, sodium phosphate buffer, 66%. [b]Conditions: (f) **16**, HBTU, DIEA, DMF; (g) i: 1 M TBAF, THF, ii: Fmoc-SPPS, and iii: TFA, TIS, H_2O; (h) TCEP, buffer, pH 6.6−6.8.

methodology in particular could be directly adapted for use in an AIP synthesis (Scheme 1B). In this approach, Fmoc-cysteine (*t*-butylthio)-OH was first coupled to PEGA resin, followed by α-amino diazotization and subsequent hydrolysis under aqueous conditions to afford an α-hydroxy cysteine resin. After chain elongation and cleavage from the resin, reduction of the cysteine side-chain disulfide led to an O to S acyl shift, resulting in α-thioester formation. Although we were able to make AIPs with this method, the isolated yields were very low (data not shown). This result highlights the crucial drawbacks of this method: the linker is synthesized on resin, and the resin options are consequently limited to those that have good swelling properties in water. To overcome these limitations, we designed a solution-phase synthesis of 2-(*t*-butyl-dimethyl-silanyloxy)-3-*t*-butyldisulfanyl-propionic acid (**16**), a molecule that acts as a masked thioester and that can be coupled onto any resin using standard approaches.

Initial efforts to generate α-hydroxy-cysteine-based linkers in solution from *t*-butylthiol protected L-cysteine proved to be unsatisfactory, primarily due to the poor yields associated with the diazotization/hydrolysis step. Therefore, we adopted an alternate route in which linker **16** was generated in five steps from commercially available thioglycerol, with an overall yield of 31%. As shown in Scheme 2, the thiol group was first protected as the *t*-butyl disulfide to give 1,2-diol **12**. Attempts to selectively oxidize the primary alcohol of **12** directly to the carboxylic acid using TEMPO[14] were unsuccessful. Instead, we protected both alcohols with *t*-butyl-dimethyl-silanyloxy (TBS) groups, followed by selective removal of the primary TBS group to give **14**. Oxidation to acid **16** was then accomplished in two steps, using Dess−Martin periodinane, followed by treatment with sodium chlorite.

Racemic linker **16** was coupled onto Rink-amide polystyrene resin with HBTU and DIEA. Following a capping procedure and on-resin removal of the TBS group with TBAF, the C-terminal residue of each peptide was attached to the resin linker using HBTU in the presence of catalytic DMAP (a double coupling procedure was typically employed). LC-MS analysis of the cleaved amino-acylated resin indicated that this loading procedure was highly efficient (i.e., no free linker was observed in the crude mixture; data not shown). Peptide-chain assembly was then performed using standard Fmoc-SPPS protocols with slight modifications for the N-methylated residues, and the peptides were cleaved from the resin with TFA (see Experimental Procedures). In all cases, LC-MS analysis of the crude cleavage mixtures revealed the presence of two closely eluting peaks, both with the mass expected for desired linear peptide-

(14) (a) Davis, N. J.; Flitsch, S. L. *Tetrahedron Lett.* **1993**, *34*, 1181. (b) Wovkulich, P. M.; Shankaran, J. K.; Uskokovic, M. R. *J. Org. Chem.* **1993**, *58*, 832.

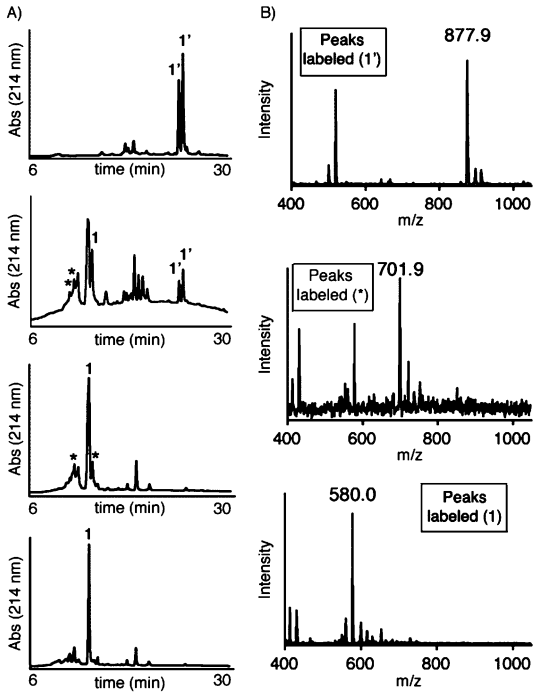

Figure 2. Cyclization reaction of crude truncated AIP-II (**1′**). (A) HPLC chromatograms of the reaction mixture at 0, 5, 80, and 230 min time points, from top to bottom. The gradient used was 15−90% B (see Experimental Procedures) in all four runs. The starting material appears as two peaks, corresponding to two diastereomers of the linker. At least three of the reaction intermediates correspond to the fully reduced linear peptide, indicating that the linear thioester is present. The linker is cleaved during the cyclization to give one product peak. (B) Mass spectra of the peaks indicated by the corresponding symbols or numbers. 877 Da corresponds to the mass of the linear starting material **1′**, 701 Da corresponds to the fully reduced peptide, and 580 Da is the mass of the cyclic product, **1**.

linker products. The top panel in Figure 2A shows the crude cleavage mixture obtained for the linear precursor to peptide **1**, which we will refer to as **1′**. We reasoned that the two products likely corresponded to the two expected diastereomers that result from use of the racemic linker. No attempts were made to purify these putative stereoisomers since the linker would eventually be cleaved off during the cyclization reaction. Indeed, incubation of crude peptide **1′** in an aqueous buffer containing the reducing agent TCEP resulted in the collapse of the two peaks into a single new peak with a mass consistent with the desired thiolactone peptide (Figure 2 and Table 1). Homonuclear ^{1}H 2-D NMR analysis confirmed that the reaction product was peptide **1** (full chemical shift assignments of all peptides prepared in this study are given in the Supporting Information). Note, the 2-D ^{1}H− TOSCY spectrum of purified **1** was identical to an authentic sample of trAIP-II prepared by our previous Boc-SPPS route (see Supporting Information).

The macrocyclization reaction was found to be the most efficient between pH 6.6−6.8, taking ∼1−2 h to reach completion. If the pH was lowered, we observed mostly a reduced version of peptide **1′** with decreasing amounts of product formation, presumably due to slower O to S acyl shift, while at higher pH values, hydrolysis to give the free α-carboxy-peptide became increasingly problematic. The use of TCEP as the reducing agent was also critical since it did not react with the thioester-containing product to an appreciable degree. In contrast, use of thiol-based reducing agents led to the generation of the corresponding linear α-thioester peptides in addition to the desired thiolactones (data not shown). Analysis of the reaction mixture after 5 min revealed the presence of several intermediates with a mass consistent with the fully reduced version of peptide **1′** (Figure 2B). Presumably, one of these intermediates corresponds to the linear α-thioester generated in situ following the O to S acyl shift, although this is likely a minor component due to the greater stability of oxyesters over thioesters.[15] Given that acyl transfer from a hydroxyl group to a thiol group is highly unfavorable, we favor the mechanism shown in Scheme 2B, in which the linear α-thioester peptide is an obligatory intermediate leading to the final transthioesterification step, which acts as a thermodynamic sink in the process. Consistent with this mechanism, efficient cyclization of the linear peptides was observed only when both thiol groups were reduced. For example, the linear precursor to peptide **11**, which has an unprotected N-terminal thiol group and protected linker thiol group, could be cyclized only in the presence of TCEP. Thus, the N-terminal thiol attacks only the thioester that is generated by deprotection of the linker and subsequent acyl shift (see Supporting Information).

Using the general procedure shown in Scheme 1B, we were able to generate all but one of the desired thiolactone peptides in good yield and purity (Table 1 and Supporting Information). The sole exception was peptide **8**, which contains *N*-methylphenylalanine at its C-terminus. Attempts to synthesize the linear precursor to this peptide by Fmoc-SPPS on linker **16** led to low yields, and the crude mixture contained significant amounts of deletion products lacking the last two residues, Leu and *N*-Me-Phe. We attribute these problems to diketopiperazine formation resulting from the presence of the tertiary amide at *N*-Me-Phe, a problem that is well-known for C-terminal proline-containing peptides prepared by Fmoc-SPPS[16] and that has been reported as a side reaction in the synthesis of N-methylated peptides.[17] Consequently, the α-thioester precursor to peptide **8** was generated using a Boc-SPPS strategy employing in situ neutralization chemistry[9] during the chain assembly to suppress DKP formation. Last, the lactam (**10**) analogue was prepared by cyclizing a partially protected linear peptide in solution followed by global deprotection.[3]

Structure−Activity Relationships of AIPs. A cell-based reporter assay was used to determine the inhibitory activity of each peptide against the receptor histidine kinase, AgrC.[6] Briefly, early exponential phase *S. aureus* reporter cultures of the indicated group were treated with AIP analogues **1**−**11** in the presence of a group-specific AIP agonist at a concentration (125 nM) above the EC_{90},[3,6] and the extent of *agr* activation was determined using a *β*-lactamase reporter with a colorimetric readout. To test both cognate and non-cognate *agr* inhibition by the trAIP-II analogues, group II and I reporter cell lines RN9372 and RN9222 were used, respectively. These strains lack the ability to produce AIPs but contain the AgrC-AgrA two component signaling cassette as well as *β*-lactamase driven by the *agr*-dependent P3 promoter. Representative dose−response curves for peptide **1** are shown in Figure 3, and the IC_{50} values for all the peptides against cognate (group II) and non-cognate (group I) strains are listed in Table 1. Importantly, the measured

(15) Jencks, W. P. *Catalysis in Chemistry and Enzymology*; McGraw-Hill: New York, 1969.
(16) Pedroso, E.; Grandas, A.; de las Heras, X.; Eritja, R.; Giralt, E. *Tetrahedron Lett.* **1986**, *27*, 743.
(17) Khosla, M. C.; Smeby, R. R.; Bumpus, F. M. *J. Am. Chem. Soc.* **1972**, *94*, 4721.

Table 1. Expected and Observed Masses of All Peptides Used in This Study as Well as Their Inhibitory Activities against Both Non-cognate (AgrC-I) and Cognate (AgrC-II) Receptors

	exptl mass	obsd mass ($M + H^+$)	IC_{50} (nM), AgrC-I (95% CI)	IC_{50} (nM), AgrC-II (95% CI)
1	579.2	580.0	90, (78−104)	293, (245−350)
1*[a]	579.2	579.0	260, (95−695)	230, (190−270)
2	549.2	550.7	189, (151−237)	1160, (855−1560)
3	549.2	550.0	40, (33−48)	194, (167−225)
4	519.2	520.7	77, (66−89)	238, (170−334)
5	593.3	595.0	639, (534−765)	7880, (4100−1.52×10^4)
6	593.3	595.0	319, (284−357)	1050, (795−1380)
7[b]	593.3	595.0		
8[b]	593.3	595.0		
9	504.2	505.0	1141, (799−1630)	5.07×10^5, (5.41×10^4 to 4.76×10^6)
10	562.3	564.0	1390, (1250−1560)	1.67×10^5, (9.64×10^4 to 2.88×10^5)
11	522.2	524.0	1680, (1310−2170)	4.73×10^4, (3.37×10^4 to 6.63×10^4)

[a] **1*** are data obtained for peptide **1** made by Boc chemistry. [b] IC_{50} values for peptides **7** and **8** could not be determined due to lack of inhibition up to the highest concentrations tested (>30 μM).

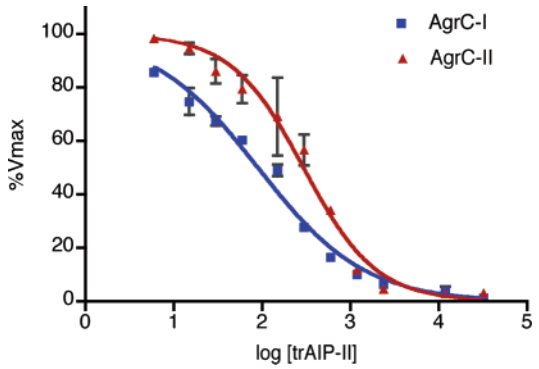

Figure 3. Inhibition curves for truncated AIP-II (**1**) in the presence of 125 nM agonist. V_{max} is the initial rate of nitrocefin cleavage by the β-lactamase reporter measured by absorbance of the hydrolyzed lactam. The error bars show the standard deviation from the mean for the two V_{max} values obtained for each concentration point.

IC_{50} values for peptide **1** prepared by our new Fmoc-SPPS route were in good agreement with those previously determined for this peptide.[4]

There are several interesting trends within the activity data summarized in Table 1. First, the overall rank order of the peptides, in terms of their inhibitory activities, is remarkably similar for the cognate and non-cognate *agr* groups, although there are nuances to this that we comment on next. Second, all of the peptides that had a measurable activity are more potent antagonists of the non-cognate AgrC receptor than of the cognate receptor. Furthermore, this difference in inhibitory activities against the two receptors increases significantly for the less potent analogues. This trend is more clearly seen in Figure 4, which shows a log−log plot of IC_{50} values. Thus, antagonism of the non-cognate *agr* group is much more tolerant to changes in the AIP structure than is antagonism of the cognate group. For instance, replacement of the thiolactone in **1** with a lactam (**10**) leads to a modest decrease in the non-cognate IC_{50} (~15-fold) relative to the effect of this change on the cognate activity (~500-fold). Similarly, replacement of the two serine residues in **1** with a methylene linker (**9**) resulted in a ~13-fold versus 1700-fold reduction in non-cognate and cognate activities, respectively.

Modifications to the serine residues in peptide **1** were well-tolerated. Both the single and the double glycine mutants (2−4) resulted in a minimal loss of activity (<5-fold) and in some cases actually increased potency (Table 1). Moreover, N-methylation of the serine residues (5 and 6) was for the most part tolerated, although cognate inhibition was somewhat sensitive to N-methylation of serine 2. In contrast, N-methylation of Leu or Phe residues (7 and 8) resulted in a complete loss of activity, further highlighting the functional importance of this region of the molecule.

The replacement of the sulfur with an NH, to give lactam **10**, had a similar effect on function as a replacement of both serines with a methylene linker to give **9** (Table 1). Thus, although the thiolactone linkage is not necessary for inhibition by full-length AIP-II, the lactam substitution is not tolerated well in the context of the truncated AIP. The relatively low activity of peptide **9** cannot be explained by the loss of the serine side chains in accordance with the activity data for peptide **4** (Table 1). It is more likely that the complete loss of one amide bond or the increased flexibility introduced by the methylene linker is responsible for the reduced potency.

Last, the removal of the N-terminal amide group caused a dramatic loss of inhibitory activity against both cognate (~250-fold) and non-cognate (~55-fold) strains. This result shows that the N-terminal vestige of the macrocyclic ring is in fact important for inhibition.

We next explored as to whether the differential activity of our analogues in any way correlated with the solution structure of the peptides, as measured by ^{1}H NMR chemical shifts around the macrocycle. Figure 5A shows a plot of the global CSI for each analogue **2**−**11** as compared to the parent peptide **1**, in order of peptide potency. While this simple analysis does not report on the receptor bound conformation of the peptides, we nonetheless saw no clear trend between potency and overall chemical shift perturbations. For instance, N-methylated peptides **7** and **8**, which have no measurable activity, have CSI values comparable to peptides **3** and **4**, which are the most potent AIP analogues. Similarly, the chemical shifts around the macrocycle in peptide **11** are largely unperturbed as compared to **1**, yet this analogue is one of the least potent antagonists. One interpretation of the previous information is that the exocyclic and two C-terminal amides of trAIP-II, which are perturbed in peptides **11** and **7**−**8**, respectively, make specific contacts with the AgrC receptor. However, we cannot rule out the possibility that these modifications prevent the AIP from assuming a bioactive conformation required for receptor binding. The largest CSI observed is for the lactam analogue **10**. In this case, chemical shift changes propagate around the entire macrocycle (Figure 5 and Supporting Information), indicating that this substitution

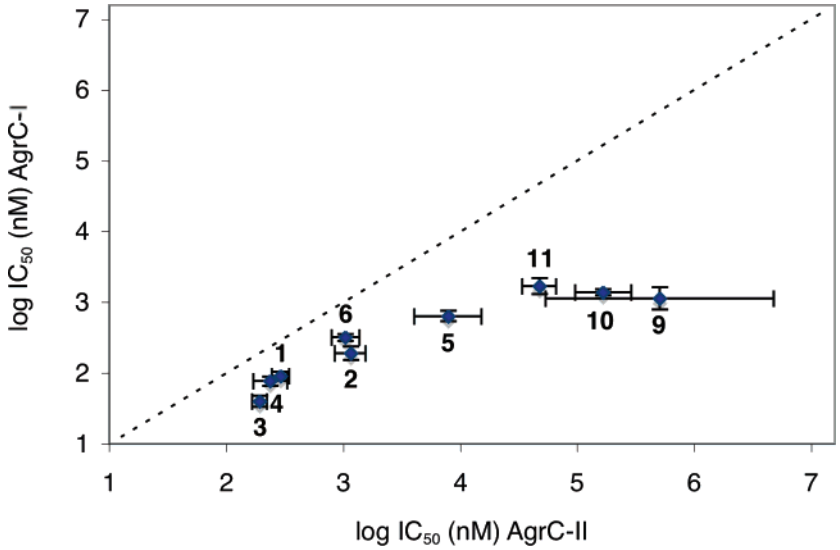

Figure 4. Log vs log plot of inhibitory activities of trAIP-II and derivatives against AgrC-II and AgrC-I. All peptides fall below the dotted black line ($y = x$), indicating that all are more active against AgrC-I than −-II. The difference in activity against the two receptors increases as the inhibitory activity decreases. The error bars represent 95% confidence intervals for each IC_{50} value.

induces far-reaching changes in the solution structure of the peptide. A similar effect was previously observed upon substitution of the thiolactone to a lactam in the context of full-length AIP.[3,6] The full-length lactam remained a potent cross-group *agr* antagonist but was an extremely weak agonist of the cognate *agr* group. Thus, whether it is agonism in the case of the full-length AIP lactam or antagonism in the case of truncated lactam **10**, the structural perturbation caused by the lactam substitution appears to significantly reduce binding to the cognate AgrC. In contrast, the presence or absence of the tail residues appears to greatly modulate the affect of the structural perturbation induced by the lactam on binding to the non-cognate receptor, AgrC-I.

The ^{1}H NMR spectra of N-methylated peptide **6** contained twice the number of resonances expected for a peptide of this size. Indeed, using standard 2-D sequential assignment methods, we found that the sample contained two species, which were present as a 1:1 mixture in DMSO-d_6 at 298 K (Figure 5B). There was no evidence for chemical heterogeneity in this peptide by LC-MS analysis (see Supporting Information). Likewise, we ruled out the possibility of these signals resulting from epimerization (i.e., C-terminal epimers) of the peptide since the same batch of amino acylated linker resins was used for the synthesis of other peptides in the study, and in these cases, no extra NMR resonances were observed, for example, peptides **3** and **4**. Further analysis of the ROESY spectrum of **6** revealed the presence of a strong NOE cross-peak between the two serine alpha protons in one of the species but not the other (Figure 5C). This cross-peak is consistent with the presence of a *cis*-amide bond between Ser2 and *N*-Me-Ser3. Analogous to the prolyl-tertiary amide, N-methylation is known to increase the propensity for trans−cis isomerization of an amide bond.[18] Two of the other three N-methylated peptides, **7** and **8**, were also present as two conformers as indicated by NMR, with the minor conformer comprising only 10−30% of the total sample population. By analogy with peptide **6**, these conformers almost certainly stem from cis−trans isomerization of the tertiary amide bond in these peptides; however, we were unable to make full assignments for the minor, presumably cis, isomers of **7** and **8** owing to their low abundance.

Discussion

In this study, we developed an efficient synthesis of *S. aureus* AIPs by employing an Fmoc-SPPS route to peptide α-thioesters. This methodology is based on the handle design of Botti et al.[12] but extends this latent thioester linker concept to any resin type. We have shown that the thiolactone-containing AIP structure can be obtained by simply incubating the corresponding protected peptide α-oxyester precursor in aqueous buffer in the presence of a non-nucleophilic reducing agent TCEP (Figure 2). Collectively, our data support the cascade-type mechanism shown in Scheme 1B, in which the reducing agent first triggers the O-to-S acyl transfer at the C-terminus, thereby setting up a transthioesterification reaction between the nascent α-thioester and the cysteine sulfhydryl to give the thiolactone, with concomitant expulsion of the linker. Although not the focus of the current study, we expect that linker **16** will be generally useful for the preparation of peptide α-thioesters for use in native chemical ligation[19] and expressed protein ligation[20] studies. Indeed, in other work, we have successfully used this linker in the Fmoc-SPPS synthesis of phosphopeptide α-thioesters for use in protein semisynthesis (T. W. Muir, unpublished results).

The staphylococcal *agr* response is responsible for integrating growth-dependent signals (i.e., quorum sensing) with a complex genetic network to coordinate the expression of a large number of virulence factors.[1] Previously, we have shown that cross-group antagonism of the *agr* response by non-cognate AIPs can be used to attenuate the spread of an infection in animal models.[3] Thus, understanding the minimal determinants of inhibition by AIP analogues is of some interest.[21] The ability to prepare AIPs

(18) LaPlanche, L. A.; Rogers, M. T. *J. Am. Chem. Soc.* **1964**, *86*, 337.
(19) Dawson, P. E.; Muir, T. W.; Clark-Lewis, I.; Kent, S. B. *Science (Washington, DC, U.S.)* **1994**, *266*, 776.
(20) Muir, T. W.; Sondhi, D.; Cole, P. A. *Proc. Natl. Acad. Sci. U.S.A.* **1998**, *95*, 6705.
(21) Gorske, B. C.; Blackwell, H. E. *Org. Biomol. Chem.* **2006**, *4*, 1441.

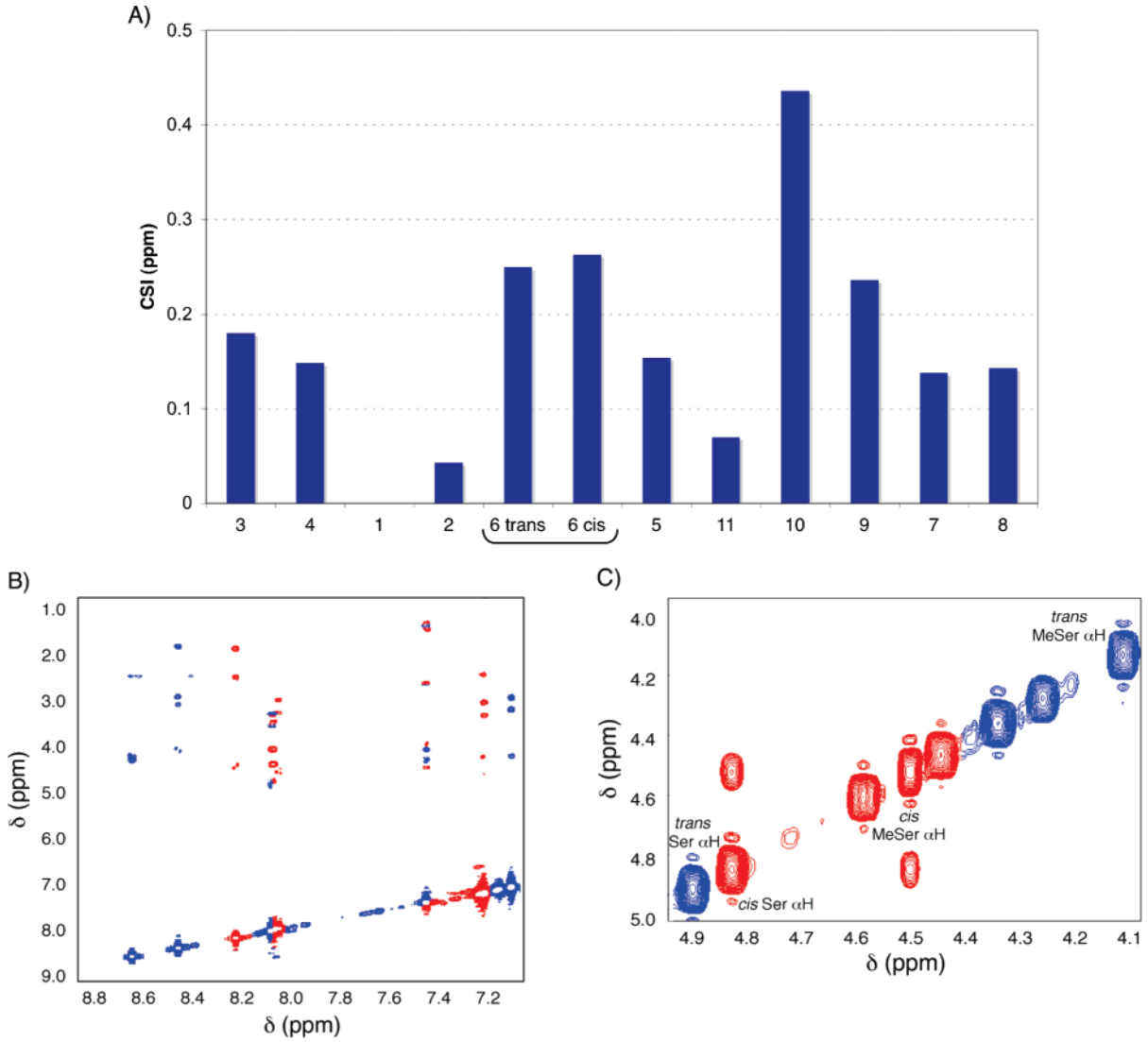

Figure 5. (A) CSI for all peptides, which are depicted in order of decreasing activity from left to right (**6** trans and cis are bracketed to indicate that they do not have two separate activities, as they are two conformers of one molecule). CSI is the average change in chemical shift relative to the NMR spectrum for **1** (see Experimental Procedures). The chemical shifts of the modified residue are excluded; thus, CSI values represent overall changes in the macrocycle beyond the site of modification. (B) Amide region of the ROESY spectrum of **6**, color-coded to identify the spin systems that correspond to each isomer. The blue and red peaks correspond to the trans and cis isomers, respectively. (C) Alpha region of the ROESY spectrum of **6**, color-coded as in panel B.

via the Fmoc-SPPS route described previously allowed us to perform a systematic SAR analysis of truncated AIP-II (**1**), which was previously found to inhibit *S. aureus* virulence of all four *agr* groups.[4]

Several interesting trends emerged from this analysis. First, the overall rank order of the analogues for cognate (AgrC-II) and non-cognate (AgrC-I) inhibition were almost identical, despite the fact that the sensor domains of AgrC-II and AgrC-I share only 31% sequence identity. However, non-cognate antagonism was more resistant to changes in AIP structure than was cognate antagonism; the former values varied by no more than ~50-fold, whereas the latter values varied by over 3 orders of magnitude (Figure 4). This observation is broadly in line with previous SAR studies on full-length AIPs, which revealed that cross-group antagonism is more tolerant to changes in peptide structure than intra-group agonism.[6] Pharmacological studies of the trAIP-II analogue have suggested that both cognate and non-cognate antagonisms operate through a simple competitive binding mechanism in which trAIP-II competes with the group-specific AIP agonist for a common binding site on the

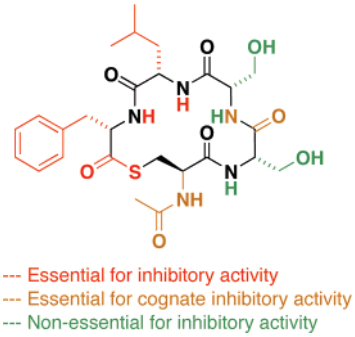

Figure 6. Peptide **1**, color-coded to indicate which portions of the structure are critical for inhibition of cognate (AgrC-II) and/or non-cognate (AgrC-I) receptors.

sensor domain of AgrC.[8c] The present SAR data are certainly consistent with this mechanism, although the details of the cognate and non-cognate interactions must be subtly different since certain modifications have a more acute effect on the former interaction than the latter (e.g., peptides **9**−**11**).

This study has allowed the principle pharmacophore for *agr* antagonism by trAIP-II, against both cognate and non-cognate AgrC receptors, to be identified. As summarized in Figure 6, one-half of the molecule that is defined by the cysteine and the two C-terminal hydrophobic residues is critical for activity. In contrast, the remainder of the molecule appears to be far less important for this activity and, in the case of non-cognate *agr* inhibition, can even be replaced by an alkyl linker without a dramatic loss of activity. This information will no doubt be useful in guiding future medicinal chemistry initiatives on this system.

Acknowledgment. We are very grateful to M. Goger for assistance with the acquisition of ROESY and TOCSY NMR spectra. We also thank Y. Wei for help with TOCSY NMR. Thanks to M. Vila-Perello, J. Cisar, and M. S. Jensen for helpful discussions. T.W.M. is a member of the New York Structural Biology Center, which is a STAR center supported by the New York State Office of Science, Technology, and Academic Research. The Q-TOF Ultima mass spectrometer (University of Illinois at Urbana−Champaign) was purchased in part with a grant from the National Science Foundation, Division of Biological Infrastructure (DBI-0100085). This work was supported by the U.S. National Institutes of Health (Grant R 501 AI42783).

Supporting Information Available: Plots of inhibitory activities of all peptides. Experimental evidence for proposed mechanism of thiolactone formation. HPLC and MS characterization and NMR chemical shift assignments of all peptides. ^{1}H and ^{13}C NMR spectra of linker **16**. This material is available free of charge via the Internet at http://pubs.acs.org.

JA711126E